Effects of Wingtip-Mounted Propellers on Wing Lift and Induced Drag

MELVIN H. SNYDER JR.* AND GLEN W. ZUMWALT†
Wichita State Universiy, Wichita, Kansas

It is proposed that aircraft can be designed using propellers at the wingtips in such a way that the L/D ratio can be varied by changing the effective aspect ratio in flight. An experimental program testing a wing with propellers mounted at the wingtips is reported. It is shown that the use of a propeller at the wingtip, turning in the direction opposite to that of the wing vortex, shifts the trailing vortex core outboard, decreases the wing drag coefficient, increases the maximum lift coefficient and increases the effective aspect ratio. Rotating the propeller in the opposite direction has the reverse effect. A functional relationship is shown to exist between $\Delta C_D/C_D$ and $T_c d^2/C_L S$.

Nomenclature

A = aspect ratio
a,a' = propeller angular velocity factor (Ref. 5)
b = span of wing (or other lifting surface), ft
b_v = vortex span, ft
C_D = coefficient of drag, D/qS
C_{D_i} = induced drag coefficient
C_{D_p} = equivalent parasite drag coefficient
C_L = coefficient of lift, L/qS
$C_{L_{max}}$ = maximum lift coefficient
$C_{L\alpha}$ = slope of lift curve, $dC_L/d\alpha$, per deg
C_Q = torque coefficient, torque/n^2d^5
D = drag; component of force parallel to the freestream velocity direction, lb
d = propeller (or impeller) diameter, ft
e_w = wing efficiency factor, $1/\pi Am$
L = lift; component of force normal to the freestream velocity direction, lb
m = slope ($\Delta C_D/\Delta C_L^2$) of straight-line fit to wing data when plotted C_D vs C_L^2
N = rotational speed of propeller rev/sec
$\mathfrak{N}$ = difference between propeller speed and windmill speed, rev/sec
R = propeller radius, $d/2$, ft
Re = Reynolds number, ft
r = radial distance, ft
r/R = nondimensional radius of a station on the propeller blade
S = wing area, ft^2
T = thrust, lb
T_c = thrust coefficient, $T/\frac{1}{2}\rho V^2d^2$
V = velocity, fps
V_t = tangential velocity, fps
x = dimension parallel to wind-tunnel centerline, ft
y = dimension measured spanwise from the plane of symmetry normal to tunnel centerline, ft
z = dimension normal to x and y, ft
α = angle of attack, deg
Γ = circulation, $\int_s V_s ds$, ft^2/deg
δ_f = flap deflection angle, deg
ρ = density (fluid, air), slugs/ft^3
Ω = $2\pi N$, rad/sec

Received December 4, 1968, revision received May 15, 1969. This paper is based on a Ph.D. thesis by M. H. Snyder submitted to the School of Mechanical Engineering at Oklahoma State University.

* Professor of Aeronautical Engineering. Associate Fellow AIAA.

† Distinguished Professor of Aeronautical Engineering. Associate Fellow AIAA.

Introduction

SATISFACTORY low-speed performance of aircraft is attained by use of large power plants or by use of boundary-layer control or circulation control to achieve high lift coefficients, or by a combination of these means. Although a larger percentage of aircraft, each year, is jet-propelled, most STOL aircraft (in which the thrust produced is of the same order of magnitude as the aircraft weight) are still propeller-driven aircraft. A logical method of attaining good low-speed performance would be the use of the installed power to augment the lift, through circulation control, in such a way as to vary the drag independently of the lift. The possibility of controlling the L/D ratio, through control of the C_{D_i}, is an attractive prospect to an aircraft designer.

The use of a finite-span lifting wing produces effects which are often considered undesirable. These effects include: 1) induced drag; 2) loss of lift near wingtips, resulting in a lower total lift, at a given angle of attack, than would be expected from two-dimensional wing-section characteristics because the maximum lift coefficient is lower than that of the wing section; 3) angle of flow at the tail plane which is not constant, but which is a function of the wing C_L.

The "traditional" method of attacking these effects has been to use end-plates, tip-tanks, or other end-bodies. It is easy to show that this method is an inefficient use of the end-body material; a low D/L would result if the material were simply used as an extension of the wing. Clements[1] reported tests on variable incidence, variable camber end-plates. Even these sophisticated end-plates can be shown to be ineffective use of the end-plate material.

Rather than manipulate wing geometry to approach two-dimensional flow, it would seem logical to use some energy source for the task of directing the flow. The most obvious source of energy is the main aircraft power plant. Objectives of controlling wing loading and downwash include high $C_{L_{max}}$, low values of induced drag (for takeoff and climb), and high values of induced drag (for approach and landing). Other design objectives are to add no weight or structural penalty, to add no additional profile drag increment, and to add no complexity to the control of the aircraft.

A proposed solution is to place at the wingtips the propellers which propel the aircraft. There are several possible advantages.

1) The rotational component of the propeller slipstream is available for amplifying or attenuating the wing vortex system. This component has, heretofore, been considered to

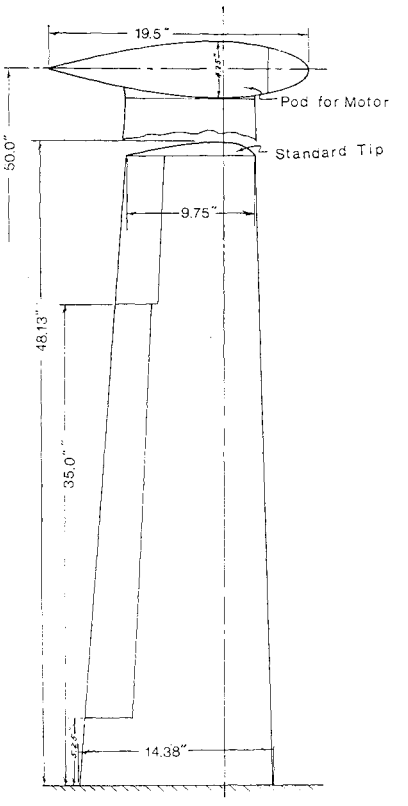

Fig. 1 Wind-tunnel model showing alternate tips.

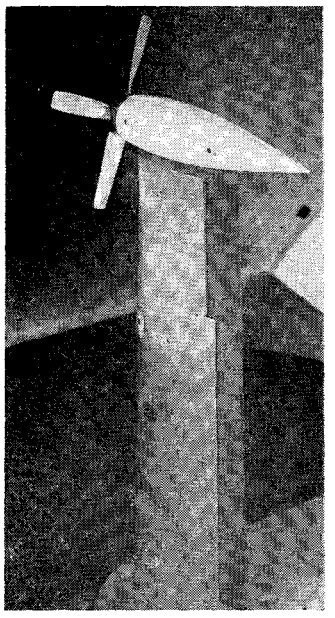

Fig. 2 Reflection-plane wind-tunnel model with tip-mounted nacelle and propeller.

represent lost energy. 2) The propellers are necessary for propulsion of the aircraft, i.e., this is not a case of adding a piece of equipment or structure; rather it is a case of locating it to best advantage. 3) Placing the engines and propellers at the wingtips will relieve the wing shear and bending moments and could result in a lighter structure. 4) Placing the engines at the wingtips and the fuel in the outboard parts of the wings would greatly improve the safety and chances for crew survival in cases of crash landing.

Possible disadvantages of this arrangement include: 1) difficulty (or impossibility) of trimming the aircraft for one-engine-out operation; 2) production of aeroelastic problems created by the changing of the torsional moment of inertia of the wing and the interaction of bending and torsional modes of flutter or vibration.

Most recent work on the effect of propeller slipstreams has considered the axial velocities only and has neglected the effects of rotation. Design of STOL aircraft using large diameter propellers having high thrust is based on the increased local dynamic pressure of the slipstream over the wings and on boundary-layer control effects of the slipstream.

The rotation of the propellers should be considered. It should be possible to combine the swirling of a propeller slipstream with the trailing wing vortex in ways such that the wing loading would be affected and the induced drag either increased or decreased.

This concept is not a new one. It has been reported that Vought Aircraft built a World War II fighter designed by Charles Zimmerman which utilized this principle. Attempts to obtain data on this plane have been unsuccessful. The efficiency of the concept has been debated, but it has not previously been systematically tested. For this reason, a wind-tunnel test was conducted to evaluate the effectiveness of the idea.

Experiment

The model tested[2] was a reflection-plane model of an aspect-ratio-8 wing. The model is shown in Figs. 1 and 2. Two propellers were used in the tests; one was a standard four-bladed propeller of relatively high efficiency (high ratio of axial velocity to angular velocity) and the other had fairly high rotational velocity compared to the axial velocity. The purpose in using this second propeller was to obtain data bearing on the observations of A. Lippisch. He stated that a limitation to the use of a propeller in affecting the wing trailing-vortex was the efficiency of the propeller; about 80% of the energy provides axial acceleration of the air and only about 20% is available to produce rotation with which to supplement or to counteract the trailing vortex and the attendant downwash pattern.

The two propellers are shown in Fig. 3. Earlier tests of an impeller (shaped something like an orange juice extractor) had shown that the device does produce thrust, but the propulsive efficiency peaks at less than 50% (according to Lippisch, then, $\frac{1}{2}$ of the energy to this propeller is used to produce rotation). This type of propeller was chosen to serve as the inefficient propeller for these tests. The "orange juicer" is referred to as the impeller and the four-bladed propeller is called the propeller. The impeller has the same basic contour as the propeller spinner. Added to that contour are twelve radial blades. The propeller is a right-hand rotation propeller. The pitch angle of the propeller blades was arbitrarily set at 15.5° (at $r/R = 60\%$). This angle corresponds to a very low pitch. Propeller activity factor is about 90 per blade.

Test Results

The principal results expected from the experimental program were: 1) alteration of the flowfield downstream of the wing; this changed flowfield would be identified by changes in the downwash and by altered trajectories of the core of the trailing vortex; 2) changes in the wing loading, resulting in changed lift-curve slope and $C_{L_{max}}$; 3) changes in wing drag, chiefly in the induced portion of the drag.

The trajectory of the core of the trailing vortex was determined from photographs of a tuft grid mounted at various

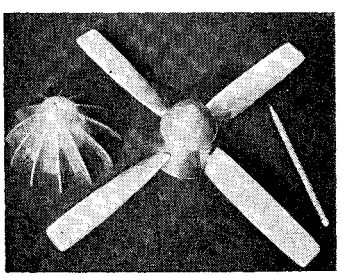

Fig. 3 Impeller and propeller.

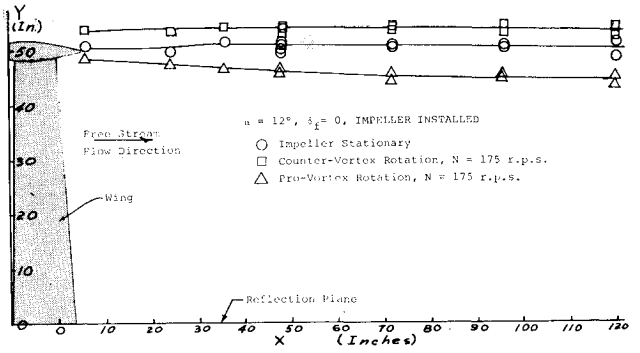

Fig. 4 Trailing vortex core trajectory in X-Y plane.

downstream positions. Figure 4 shows the trajectories of three trailing vortices in the X-Y plane. The model configuration is the wing with the impeller installed at the tip; $\alpha = 12°$, $\delta_f = 0°$. At more than one semispan downstream, with

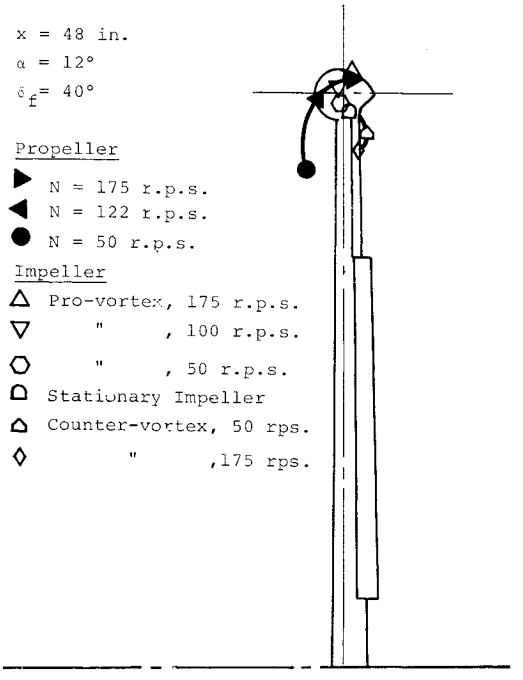

Fig. 5 Effect of rotor speed and direction on position of vortex core one semispan downstream.

no rotation of the impeller the vortex span is 101 in.; counter-vortex rotation shifts the vortex outboard to a vortex-span of 107 in.; vortex-direction rotation reduces the vortex-span to 89 in.

Figure 5 shows the position of the center of the vortex core at a distance of one semispan downstream of the trailing-edge

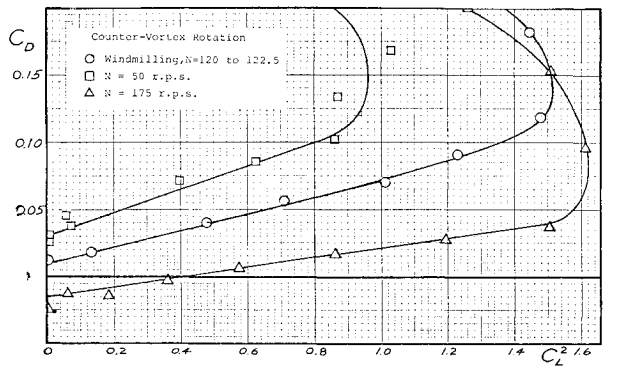

Fig. 6 Drag polar, corrected for propeller thrust.

Table 1 Vortex span and effective aspect ratio

Configuration	Eff. aspect ratio Ae_w	Vortex span b_v, ft
Dummy spinner, no propeller	6.45	8.25
Stationary impeller	6.32	8.42
Impeller, N = 175 rev/sec	10.35	8.93
Impeller, N = −175 rev/sec	5.34	7.42
Propeller (windmilling), N = 122 rev/sec	5.73	8.33
Propeller, N = 175 rev/sec	10.1	8.42
Propeller, N = 50 rev/sec	4.0	7.42

(The positive direction of rotation is that of the propeller—counter vortex. When N is negative, the rotation is in the vortex direction.)

for most of the configurations tested. The wing was at an angle of attack of 12° and with the flaps deflected 40°. The following results can be detected.

1) Adding the pod moves the trailing vortex outboard compared to the wing with a standard tip. 2) Counter-vortex rotation of the impeller and counter-vortex rotation of the propeller (at greater than windmilling speed) moves the vortex outboard. 3) Vortex rotation of the impeller and counter-vortex rotation of the propeller at less than windmill speed causes the vortex to move inboard. 4) In the range of rota-

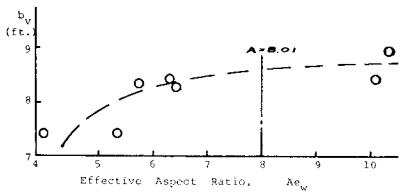

Fig. 7 Vortex span and effective aspect ratio for test configurations.

tion speeds involved, the propeller produces greater shift of the trailing vortex than does the impeller.

The change in the vortex span is apparent in Figs. 4 and 5. It can be seen that the change in vortex span is not the result of bending of the flow downstream of the wing. Rather, the shift apparently occurs upstream of the first tuft-grid position. This fact indicates that the vortex span is the result of the distribution of strength in the shed vortex sheet.

Table 1 summarizes the vortex span and the effective aspect ratio for the various configurations tested. The effective aspect ratio was determined from the slope of curves such as Fig. 6. The relation between vortex span and effective aspect ratio is shown graphically in Fig. 7. Three-component balance data were taken and corrected for direct-thrust of the impeller or propeller. Table 2 summarizes the principal results.

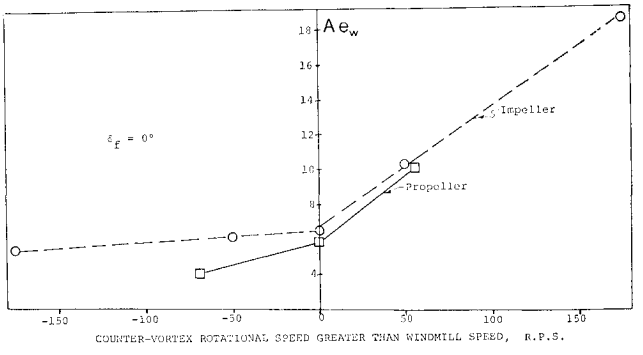

Fig. 8 Variation of effective aspect ratio caused by rotor speed.

Table 2 Summary of wing characteristics

δ_f, deg	Rotation Direction	N, rev/sec	$C_{L_{max}}$ Not cor.	$C_{L_{max}}$ Cor. for thrust	C_L Not cor.	C_L Cor. for thrust	$C_D = C_{D_p} + mC_L^2$ (cor. for thrust)	Effective aspect ratio Ae_w
	Plain wingtip							
0	None		1.22	...	0.083	...	$0.012 + 0.0477C_L^2$	6.67
40	None		1.80	...	0.08	...	$0.052 + 0.042C_L^2$	7.48
	Pod with dummy spinner							
0	None		1.25	...	0.078	...	$0.013 + 0.0493C_L^2$	6.45
40	None		1.80	...	0.093	...	$0.058 + 0.0357C_L^2$	8.91
	Impeller							
0	None		1.25	...	0.085	0.085	$0.013 + 0.0503C_L^2$	6.32
0	Vortex	50	1.26	1.215	...	0.072	$0.015 + 0.0517C_L^2$	6.15
0	Vortex	175	1.25	1.27	...	0.083	$0.0125 + 0.0595C_L^2$	5.34
0	Counter vortex	50	1.22	1.19	...	0.085	$0.015 + 0.0307C_L^2$	10.35
0	Counter vortex	175	1.31	1.26	...	0.08	$0 + 0.017C_L^2$	18.7
	4-bladed propeller							
0	Counter vortex	50	0.95	1.19	0.08	0.072	$0.032 + 0.0795C_L^2$	4.0
0	Counter vortex	119	1.2	1.22	0.085	0.08	$0.012 + 0.0555C_L^2$	5.73
0	Counter vortex	175	1.325	1.265	0.10	0.086	$0.013 + 0.0315C_L^2$	10.1

The most interesting of these results are shown graphically in Figs. 8 and 9. In each of these figures, the abscissa is the counter-vortex rotational speed of the rotor above (i.e., greater than) windmill speed. In the case of the propeller, windmill speed is approximately 120 rev/sec, so that the propeller curve is plotted for the range 40 rev/sec to 175 rev/sec (counter-vortex). In the case of the impeller, the windmill speed is zero; the negative speeds are, then, rotation vortex-direction and the positive speeds are in the counter-vortex direction.

Figure 8 shows a pronounced relationship between impeller or propeller speed and the effective aspect ratio Ae_w.

Table 2 and Fig. 9 summarize the effective aspect ratio $C_{L_{max}}$ and the induced drag due to wingtip mounted impeller or propeller. These effects were obtained by fitting straight lines to the graphs of C_D vs C_L^2 such as Fig. 6. The equation of the line $C_D = C_{D_p} + mC_L^2$.

The change in the induced drag due to wingtip rotor may be explained by Fig. 10. In the case of the vortex-direction rotation, the downwash due to the rotor combines with the wing downwash to produce greater downwash at the wing and an increase in the induced drag. Figure 10 also shows that a counter-vortex rotation of the rotor produces a smaller downwash at the wing, and a smaller induced drag.

In the terms of trailing vortex strength, the vortex-direction turning rotor may be called a "vortex source," and the counter-vortex turning rotor may be called a "vortex sink." "Vortex source" and "vortex sink" were used in this sense by M. Roy, Director of the Office National d'Etudes et de Récherches Aerospatiales.

These functions are the results of the rotating vortex sheet downstream of the propeller which is superimposed on the shed vortex sheet of the wing. The wing vortex sheet is thus attenuated or amplified. It is possible to conceive of counter-vortex rotating propellers distributed along a wing of sufficient strength to absorb completely the vortices shed by the wing, resulting in infinite effective aspect ratio.

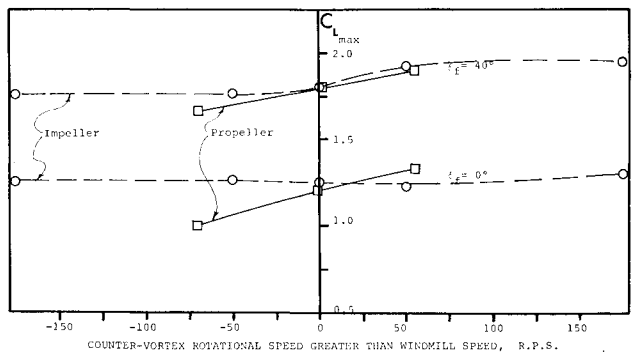

Fig. 9 Effect of rotor speed on $C_{L_{max}}$.

Comparison with Conventional Aircraft

For comparison with the test results, data have been extracted from Refs. 4 and 5 on the RM-9 airplane. This four-engine midwing airplane was equipped with the same wing as the wing of this test, except that it was equipped with four engine nacelles, two on each wing. Some effects of power are listed in Table 3. Propellers 1 and 2 are on the port wing and turn in the same direction as the shed vorticity. Propellers 3 and 4 turn in the direction opposite to that of the shed vorticity of the starboard wing.

These data confirm that the C_L slipstream is higher than without a slipstream, even without including any lift component of the thrust. They also confirm the fact that it is better to turn the propellers in the direction opposite to the direction of the vortices being shed. This effect is shown by the slope of the curves in Fig. 11, which also indicates that the

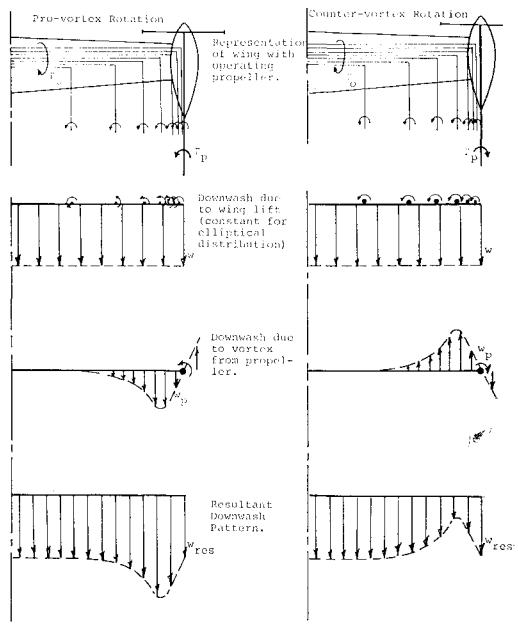

Fig. 10 Change of downwash pattern due to propeller-produced tip vortex.

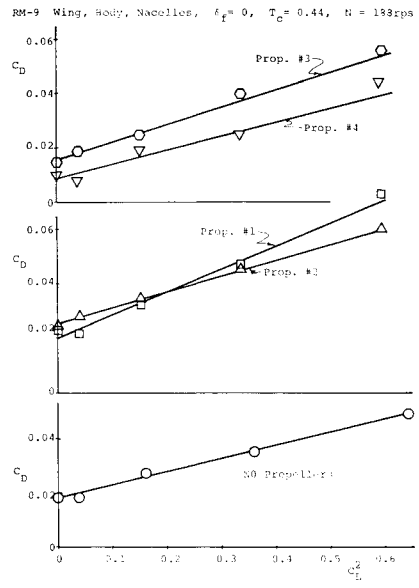

Fig. 11 Effect of propeller position on drag polar.

effect is more marked for propellers near the wingtip than it is for inboard propellers. Propellers 1 and 4 are outboard and 2 and 3 are inboard propellers. Both the ΔC_L and the change in $dC_D/dC_L{}^2$ due to propeller action are only partly due to increased slipstream velocity. They are also due to the amplification or attenuation of wing lift due to interaction of the rotating propeller slipstream with the wing.

Figure 11 indicates a similar effect with a single impeller or propeller mounted at the wingtip; i.e., as the counter-vortex speed of the rotor increases, the value of $C_{L_{max}}$ increases.

To analyze further the effect of spanwise propeller position, additional data were abstracted from Ref. 4. The values of effective aspect ratio, lift-curve slope, and D/L at $C_L = 1.0$ are plotted in Fig. 12.

Figure 12 illustrates the effects of spanwise position of the propeller on the wing performance. In each case listed, there is only one propeller operating; it is operating at a spanwise position listed. All points plotted correspond to N = 175 or 188 rev/sec and T_c = 0.42 or 0.65, except the ones corresponding to the left-hand wingtip [$y/(b/2) = -1.0$]. These points are for the propeller turning in the counter-vortex

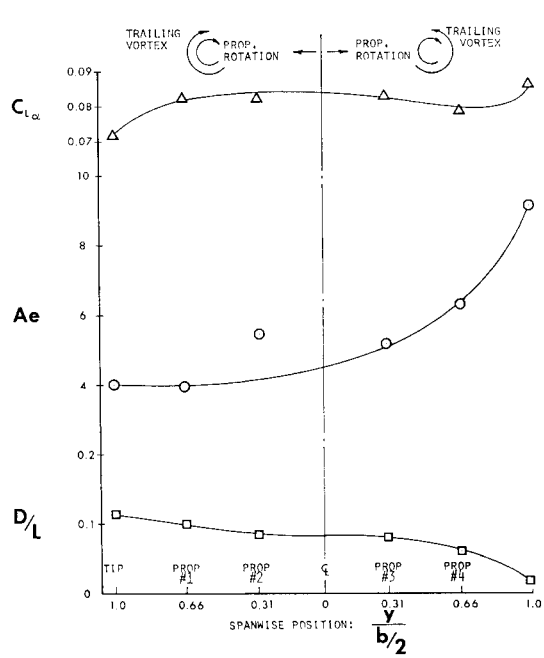

Fig. 12 Effect of propeller position on wing characteristics.

Table 3 RM-9 with 60 deg flaps, no tail[a]

Configuration	C_L at $\alpha = 0°$	$C_{L_{max}}$
No propellers	0.93	1.77
Propellers 1 & 2 only, $T_c = 0.82$	1.33	2.38
Propellers 3 & 4 only, $T_c = 0.82$	1.47	2.50
All propellers, $T_c = 0.82$	1.80	3.40

[a] $Re = 7.3 \times 10^5$, direct thrust effects removed.

direction at less than windmill speed and at negative thrust (speed is about 70 rev/sec less than windmill speed, and T_c is approximately -0.8).

Generalized Results

To increase the usefulness of the results of this investigation, an attempt has been made to generalize them by examining the relationship between the strength of the vortex of the propeller and that of the wing vortex, together with the concept of the propeller acting as a vortex sink (or source) with respect to the shed vortex sheet.

Each blade of a propeller sheds a vortex sheet. This helical vortex sheet combines with those of the other blades to produce a trailing vortex system consisting of two parts—a cylindrical vortex sheet encasing the slipstream and a vortex collinear with the propeller axis of rotation. The cylindrical vortex sheet may be considered to be composed of ring vortices; the result of these vortices is that the slipstream velocity is greater than freestream velocity. The axial vortex produces the rotation of the slipstream core.

The angular velocity, according to Konig,[6] is $2a'\Omega$, where

$$a' = \frac{8C_QV}{\pi^2(1 + a)Nd}$$

The maximum tangential velocity is

$$V_{t_{max}} = \frac{16}{\pi}\frac{C_Q}{1+a}V$$

Measurements indicate that, instead of this maximum tangential velocity occurring at the propeller tip, it occurs at r/R = 0.4. V_t falls to approximately zero at $r/R = 1$.

There is, then, a trailing vortex system superimposed on the wing trailing vortex system. Schaffer[7] has shown that the vortices will combine to strengthen the trailing vortex (if they have the same sense) or to decrease the strength (if they have opposite sense).

For a given diameter, the vortex strength of a propeller will be proportional to the blade lift and, therefore, to the propeller thrust;

$$T = T_c(\rho/2)V^2d^2$$

Circulation (i.e., vortex strength of the wing) is proportional to the wing lift;

$$L = C_L(\rho/2)V^2S$$

$$\frac{\Gamma_{prop}}{\Gamma_{wing}} = \frac{T}{L} = \frac{T_c\rho/2V^2d^2}{C_L\rho/2V^2d^2} = \frac{T_cd^2}{C_LS}$$

This ratio has been used to examine $\Delta C_D/C_L{}^2$ and $\Delta C_D/C_D$. Figure 13 shows the dependence of $\Delta C_D/C_D$ on $T_cd^2/C_LS/2$. There appears to be a functional relation and a single curve has been fit to the data.

Data for the impeller is also plotted in Fig. 13. As would be expected, these data do not fit the propeller data for the reason that the rotation of the slipstream of the impeller is a direct function of N, rather than of thrust.

The parameter $\Delta C_{D_i}/C_L{}^2$ has been evaluated for various values of $\mathfrak{N}d/b$, where $\mathfrak{N}$ is the difference between rotor speed and windmilling speed. It was found that ($\Delta C_{D_i}/C_L{}^2$) varies

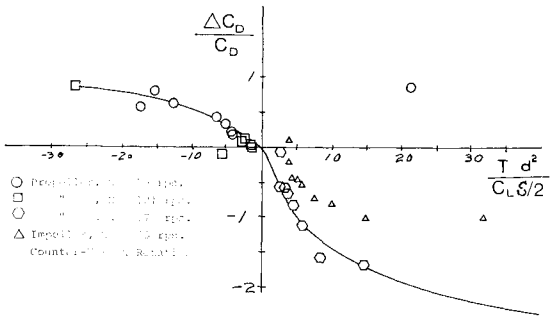

Fig. 13 Correlation of drag coefficient increment.

with the cube root of $(\mathfrak{R}d/b)$. This relation is shown graphically in Fig. 13.

Conclusions

The principal conclusion is that the use of propellers mounted at the wingtip can produce simultaneous lift increase and drag decrease. The fractional changes in both drag coefficient and lift coefficient are functions of $T_c d^2/C_L S$.

Other results of the investigation include the following.

1) Energy may be employed to affect the wing's flowfield and lift distribution by mounting the aicraft's propellers at the wingtips.

2) Use of a rotor turning in the direction opposite to that of the wing's trailing vortex shifts the core of the trailing vortex outboard and downward.

3) Use of a pro-vortex turning rotor (or counter-vortex propeller turning at less than windmill speed) moves the core of the trailing vortex inboard.

4) Wingtip configuration and/or rotor rotation have little effect on the position of the vortex trailing from the outboard end of a deflected flap.

5) There is a mutual dependence between vortex span and effective aspect ratio. As one increases, the other does also.

6) Effect of power on C_L is mainly due to higher slipstream velocity for inboard propellers. However, for propellers at the wingtips, the effect is chiefly due to the altered angle of attack in, and adjacent to, the slipstream as well as to increased slipstream dynamic pressure.

7) A counter-vortex turning propeller decreases wing drag (mainly, induced drag); a vortex-turning propeller increases drag.

8) The effectiveness of the propeller in affecting the lift and drag increases as it is moved outboard toward the wingtip.

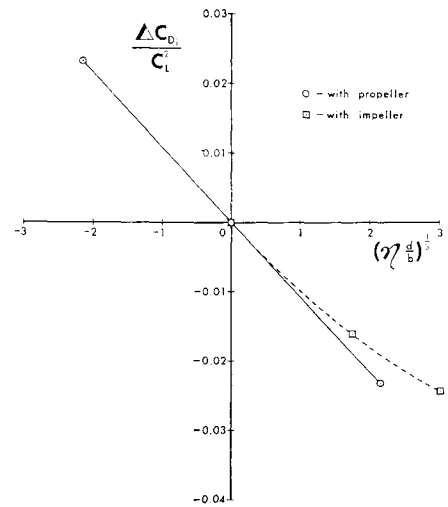

Fig. 14 Effect of propeller speed and size on induced drag coefficient.

A new experimental program is currently under way to attempt to control the shed vortex from a blowing boundary-layer control wing by the use of air jets at the wingtip.

References

[1] Clements, H. R., "Canted Adjustable End-Plates for the Control of Drag," *Aeronautical Engineering Review*, Vol. 14, No. 7, July 1955.

[2] Snyder, M. H., "Effects of Wingtip-Mounted Propeller on Wing Lift Induced Drag, and Shed Vortex Pattern," Ph.D. thesis, May 1967, Oklahoma State University.

[3] Snyder, M. H., ed., "On the Theory of Delta Wings", AR 66-4, Wichita State University, Wichita, Kansas.

[4] Stalter, J. L. and Wattson, R. K., "Effects of Power on the Aerodynamic Characteristics of a Circulation Control", Research Model, WUER 187, Pt. 2, March 1957, University of Wichita, Wichita, Kansas.

[5] Stalter, J. L., "Investgation of the Basic Aerodynamic Characteristics of a Circulation Control," Research Model, UWER 187, Pt. 1, Dec. 1956, University of Wichita, Wichita, Kansas.

[6] Koning, C., "Influence of the Propeller on Other Parts of the Airplane Structure," *Aerodynamic Theory*, Vol. IV, edited by W. F. Durand, Julius Springer, Berlin, 1935.

[7] Schaffer, A., "A Study of Vortex Cancellation," *Journal of the Aerospace Sciences*, Vol. 27, No. 3, March 1960, p. 193.